STUDY OF SUSPENSION CHARACTERISTICS USING FLEXIBLE SUBFRAME

TOMAS VRANA[1], JAN KOVANDA[2], JOSEF BRADAC[3]
[1]Department of Vehicles and Ground Transport
Faculty of Engineering, CULS Prague, Prague, Czech Republic
[2]Department of Security Technologies and Engineering
Faculty of Transportation Sciences, CTU in Prague
Prague, Czech Republic
[3]Department of Automotive Technology
Skoda Auto University, Mladá Boleslav, Czech Republic

This paper analyzes the impact of subframe flexibility of single-axle suspension on elasto-kinematic properties of axles. Geometrical parameters of the suspension, such as camber angle β and toe angle α and their change upon vertical movement of the wheel or when exposed to longitudinal and lateral forces affect very significantly driving properties of the vehicle. Using HyperWorks simulation software the computational multibody system (MBS) of axle suspension coupled with the flexible model of axle and longitudinal arms reflecting their flexibility was created. These models were developed using the method of synthesis of natural modes Craig-Bampton. The model further comprises force elements such as springs, shock absorbers and transverse stabilizer and contains nonlinear deformation characteristics of rubber-metal bushings. The effect of the subframe flefibility has been studied in several structural variants using different material. Elasto-kinematic calculations were validated by experimental measurements on measuring device for the axle alignment.

1. INTRODUCTION

Today, there are high demands related to motor vehicles not only in the field of active and passive safety as well as concerning comfort and road-holding. Driving dynamics and vehicle behavior directly affects the active safety. The mathematical description of the general computational models of vehicles used to the determination of longitudinal, lateral and vertical vehicle dynamics is published in [Poop 2010]. Driving dynamics of the vehicle is influenced by many aspects and parameters, among which belongs the elasto-kinematic behavior of axles. Therefore, high attention should be paid to this aspect. For example, the influence of suspension characteristics of the front and rear axle on the vehicle roll is published in [Shim 2010].

Elasto-kinematics of axle suspension can be defined as variation in the geometric parameters of the wheel (camber, toe angle) when the actual wheel and suspension travel during the force load in lateral and longitudinal direction of the vehicle. These courses and their changes are highly influenced by the position of kinematic points of suspension mechanism, stiffness of rubber-metal bushings as well as stiffness of structural elements such as subframe, longitudinal and transverse arms or knuckles. The stiffness of these elements can significantly influence the elasto-kinematic behavior of the axle suspension.

For kinematic analyses and synthesis of spatial suspension mechanisms the method of transformation matrices can be very suitably used such as method of disconnected closed loop or the method of body removal. Interpretation of these methods and their application to practical examples are presented in [Brat 1981].

Construction of computational models with five-unit suspension for elasto-kinematic analyzes, which take into account flexibility of kinematics pairs of each arm, is solved in [Hiller 1985] and [Knapczyk 1995]. Arms and other parts of the suspension mechanism were assumed absolutely rigid.

MBS elasto-kinematic model of single-axle suspension with five arms and Synthesis of five-link suspension is published in [Knapczyk 2006a]. Arms of the suspension mechanism were assumed absolutely rigid, bushing inclusive subframe bushings were assumed flexible. Synthesis of five-link suspension is published in [Simionescu 2002] and [Knapczyk 2006b], which also introduce new algorithms.

In publication [Heissing 2008] there are mentioned the results of elasto-kinematic simulations for rear axle suspension using MSC. ADAMS system. In this case the knuckle flexibility was taken into account. Waveforms of camber angle under the action of lateral forces for the rigid knuckle model differ by 40%. For the rigid knuckle was calculated linear change in camber of 0.07 deg / 1000 N and for flexible knuckle 0.14 deg / 1000 N. However, the validation of results is missing.

Publication [Moon 2012] presents MBS model of front single-axle suspension system also created in MSC.ADAMS. The computational model includes the model of leaf springs, which were created in MSC. Nastran and implemented into the FLEX module in MSC.ADAMS system. Other suspension components were modeled as absolutely rigid. Finally, publication [Moon 2012] shows courses of toe and camber angle for different loading modes.

Subframe of independent suspension is usually complex weldment consisting of a large number of open and closed metal profiles. It contains many kinematics points for mounting arms of suspension mechanism into the vehicle body. The subframe is deformed under the load of vertical, longitudinal and lateral forces and shifting the kinematic points with respect to the fixed coordinate system, which causes negative changes in geometric parameters of axle suspension. Consideration of subframe flexibility in the MBS model therefore plays a key role and increases the accuracy of analyzes.

This paper deals with the creation of MBS computational model of single-axle suspension using flexible subframe. Elasto-kinematic analyzes are performed for rigid and flexible model in various structural variants. Moreover, the MBS model reflects flexibility of one arm, which is necessary for the proper function of the suspension kinematics mechanism. The complex computational model of single-axle suspension was created using HyperWorks simulation software [Altair 2015].

2. MBS MODEL IN HYPERWORKS

MBS model introduces the concept of the mechanical system consisting mostly of absolutely rigid but also flexible bodies which are joined together with different types of kinematics pairs. Mutual combination between the number of objects and the type of kinematics pairs allows the system to perform a defined movement with n degrees of freedom according to the equation

$$n = 6 \cdot (u - 1) - 5 \cdot (R + T) - 3 \cdot SP, \qquad (1)$$

where u is the number of elements of axle suspension mechanism including the frame, R the number of rotational kinematics pairs (KP), T the number of sliding KP and SP the number of spherical kinematics pairs.

Each body is defined by its weight and moment of inertia. Body position in the absolute coordinate system (GCS) is defined by dependent coordinates vector **s** (2) for the number of coordinates m > n

$$\mathbf{s} = \begin{bmatrix} s_1, s_2, \dots s_j, \dots s_m \end{bmatrix}^T. \qquad (2)$$

The vector **s** consists of the position vector of the mass bodies center, $r = [x, y, z]^T$, defined by Cartesian coordinates and the orientation vector of Euler angles $\varepsilon = [\Psi, \Phi, \Theta]^T$. The mathematical tool MotionSolve in HyperWorks system assembles to calculate equations of motion

generated by the MBS model preprocessor MotionView using Lagrange equations of mixed type (equation of Lagrange multipliers) number n + r, where r = m – n. Lagrange equations are written in matrix form (3)

$$\frac{d}{dt}\left(\frac{\partial E}{\partial \dot{s}}\right) - \frac{\partial E}{\partial s} + \mathbf{J}^T\boldsymbol{\lambda} = \mathbf{Q},\qquad(3)$$

where E is the kinetic energy of the system, $Q = [Q_1, Q_2, ...Q_i, ...Q_m]^T$ the vector of generalized forces, $\lambda = [\lambda_1, \lambda_2, ...\lambda_k, ...\lambda_r]^T$ the vector of Lagrange multipliers and $\mathbf{J}^T$ matrix (4)

$$\mathbf{J}^T = \begin{bmatrix} \frac{\partial f_1}{\partial s_1} & \cdots & \frac{\partial f_k}{\partial s_1} & \cdots & \frac{\partial f_r}{\partial s_1} \\ \vdots & \cdots & \vdots & \cdots & \vdots \\ \frac{\partial f_1}{\partial s_j} & \cdots & \frac{\partial f_k}{\partial s_j} & \cdots & \frac{\partial f_r}{\partial s_j} \\ \vdots & \cdots & \vdots & \cdots & \vdots \\ \frac{\partial f_1}{\partial s_m} & \cdots & \frac{\partial f_k}{\partial s_m} & \cdots & \frac{\partial f_r}{\partial s_m} \end{bmatrix}.\qquad(4)$$

The individual elements of $\mathbf{J}^T$ matrix arise as the partial derivation of relevant constraints listed in the matrix form (5) according to elements of dependant coordinate vector s

$$f = (s,t) = 0.\qquad(5)$$

The number of constraints and Lagrange multipliers is r. The kinetic energy of the system is a function of dependent coordinate vector s and the time t. E = E (s, s, t) value is determined as the sum of kinetic energies of individual elements [Stejskal 2001].

Lagrange equations (3) represent a set of differential-algebraic equations (DAE), which are difficult to solve analytically. MotionSolve is looking for the unknown vector of dependent coordinate s using numerical mathematics, so called DSTIFF integrator whose basic principle is based on common numerical method DASPK.

3. COMPUTATIONAL
MBS MODEL OF SINGLE-AXLE SUSPENSION
Preprocessor MotionView of HyperWorks system was used to generate the MBS model of single-axle suspension (Fig. 1). This model was subsequently used for elasto-kinematic analyses.

Suspension mechanism of the axle was created according to kinematic scheme in Fig. 2.
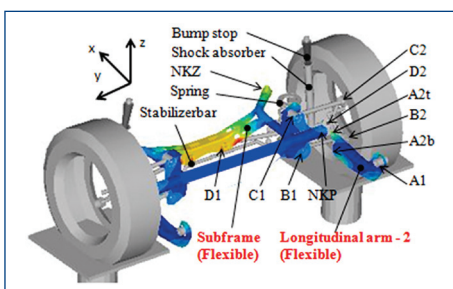
Figure 1. MBS computational model with implemented FEM models
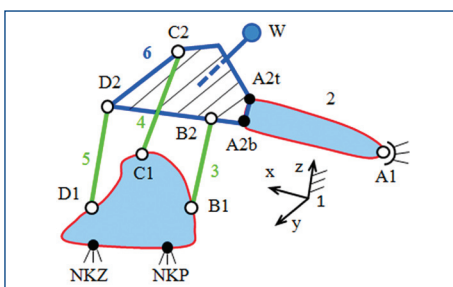
Figure 2. Suspension kinematic scheme

Knuckle 6, to which is firmly connected the wheel center point W is in kinematic points A2t, A2b, B2, C2 and D2 connected to the frame 1 by means of four arms (bodies 2, 3, 4, 5). In kinematic points A2t, A2b between knuckle 6 and the longitudinal arms 2 kinematic pair type FIX was used (takes 6 DOF). At points B1, B2, C1, C2, D1 and D2 transverse arms 3, 4 and 5, the BALL joint type (takes 3 DOF) was applied. Subframe is connected with an absolutely rigid frame (Ground body) at points NKP, NKZ using FIX type joint.

Position of kinematic points of the left suspension mechanism in GCS shows Table 1. The right side is symmetrical about the x axis. Particular mass, inertia and center of gravity have been defined for individual bodies.

Point of suspension kinematic pair	Coordinates in GCS		
	x [mm]	y [mm]	z [mm]
A1	2098	−603	36
A2t	2402	−595	27
A2b	2402	−595	−33
B1	2480	−365	−21
B2	2502	−678	−40
C1	2534	−380	143
C2	2540	−685	130
D1	2805	−105	−10
D2	2790	−685	−45
NKP	2410	−482	72
NKZ	2860	−485	95

Table 1. Position of kinematic pairs in absolute coordinate system (GCS)

The model also includes a helical spring with linear stiffness of 29 N/mm, transverse stabilizer with diameter of 20 mm, shock absorber and rubber bumper defined by the progressive deformation characteristics. These elements cause additional stress and deformation of the supporting elements of the suspension and thus affect its elasto-kinematic behavior. Therefore, it is very important to implement them into computational models of elasto-kinematics characteristics.

The deformation behavior of real rubber-metal bushings is in the MBS model replaced by kinematic pairs with defined flexibility. That is for each bushing described by non-linear deformation characteristics. There are six cases of elementary bushing load (Fig. 3). There are two radial deformation characteristics Dx = f (Fx), Dz = f (Fz) and one axial Dy = f (Fy). Furthermore, there are two cardanic torque characteristics φz = f (Mz), φx = f (Mx), and one torsion φy = f (My).
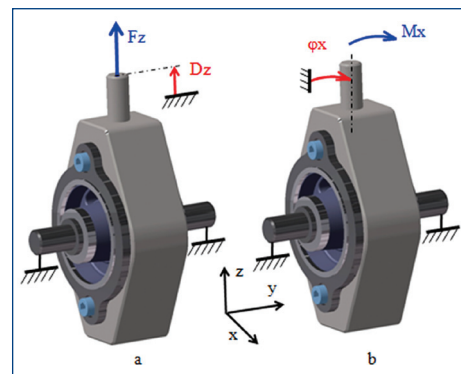
Figure 3. Measuring deformation characteristics of rubber-metal bushings using preparatory equipment, a – radial characteristics Dz = f (Fz), b – cardanic characteristics φx = f (Mx)

Relevant characteristics of individual bushings were found by experimental measurements using specially designed measuring head. This head is equipped with removable element for different bushing diameters of individual suspension arms.

3.1 Subframe flexible model

FEM model of subframe 1 and model of longitudinal arm 2 (Fig. 1) were implemented into MBS model with rigid bodies. FEM models were created in Hypermesh preprocessor, most commonly used to prepare models for static and dynamic calculations using finite element method.

Models were imported into Hypermesh in the form of surface CAD models through the neutral format STEP. In this environment, the models were discretized and thus the combined FEM network consisting of quadrilateral and triangular surface elements PSHELL type was created. Subframe network consists of 24309 nodes and 24238 elements of an average size of 5 mm (Fig. 4).
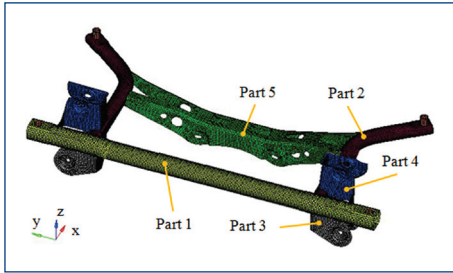
Figure 4. MKP model of subframe with definition of individual parts

Geometric edges and entities that occur during CAD surface modelling and adversely affect the final quality of the network were removed. In this paper, there were created individual structural variants of subframe. Then the effect on elasto-kinematic properties of single-axle suspension has been studied. All created and analyzed subframe variants are shown in Table 2. Two basic materials were chosen for the analysis. Steel with density ρ = 7 850 kg/m³, Young modulus E = 2.1·10⁵ MPa and Poisson number μ = 0.3 and aluminium alloy AlSi7Mg with Young modulus E = 0.74·10⁵ MPa and Poisson number μ = 0.33 according to [Michalec 1995].

Variant	Plate thickness [mm]				
	Part 1	Part 2	Part 3	Part 4	Part 5
V1-steel	3.5	3.0	3.0	2.5	3.0
V2- steel	3.5	3.0	3.0	2.5	2.0
V3- steel	3.5	3.0	2.0	2.5	3.0
V4- steel	3.5	3.0	3.0	1.5	3.0
V5- steel	3.5	2.0	3.0	2.5	3.0
V6- steel	2.5	3.0	3.0	2.5	3.0
V1-AlSi7Mg	3.5	3.0	3.0	2.5	3.0
V2-AlSi7Mg	6.0	5.0	5.5	4.5	5.0

Table 2. Variants of subframe flexible model

These mechanical properties of materials were assigned to each network element. Other subframe variants were prepared by assigning different thicknesses for individual subframe elements. Fig. 4 shows cross bar (1), longitudinal bar (2), lower and upper bracket (3, 4) and transverse profile (5). In order to assign elements for different thicknesses, the network elements in the simulation model were classified into appropriate groups. The model of longitudinal arm was always assigned to steel and the thickness of 3.0 mm.

Flexible models in H3D format were generated by the synthesis of modal modes using Craig- Bampton method, which is processed in FLEXPREP tool of MotionView module. The input of FLEXPREP is the FEM model exported from Hypermesh and RBE2 spiders. Craig-Bampton method approximates the linear displacement vector of network nodes **u** using linear combinations of matrices of modal mode **K** and modal coordinate vector **q** according to equation (6)

$$\mathbf{u} = \mathbf{K} \cdot \mathbf{q}(t). \tag{6}$$

Presumption of this relationship is small linear deformation of the modal flexible body. This flexible model can relatively move to the GCS together with MBS model. Position vector of flexible body $\mathbf{r}_{fl}$ (Fig. 5) is extended in comparison to the conventional position vector of absolutely rigid body with the vector of displacement nodes **u** according to equation 7.

$$\mathbf{r}_{fl} = \mathbf{r}_{0b} + \mathbf{T}_{0b} \cdot (\mathbf{r}_T + \mathbf{u}), \tag{7}$$

where $\mathbf{r}_{Ob}$ is the position vector of the local coordinate system of the body, $\mathbf{T}_{0b}$ the matrix of directional cosines of local systems to the global system, $\mathbf{r}_T$ is the position vector of nodes in the local system of the body before its deformation and **u** is the vector of displacement nodes of deformed body network.
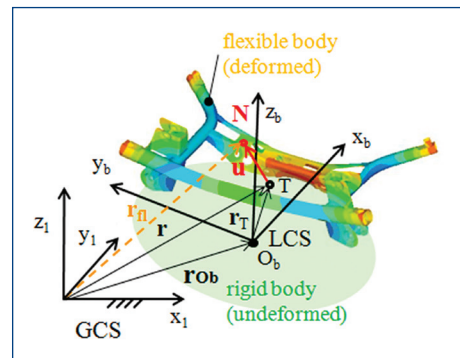
Figure 5. Position vector of modal flexible body

Time derivation of equation (7) produces the velocity vector of flexible body, which is the input of Lagrange equations when calculating the MBS model that contains the flexible body.

Sufficiently precise deformation of real components can already be achieved using low number of modes of modal flexible body. Required number of modal modes describing the deformation of the body is determined from the modal analysis which proceeds in MotionView module. The first three calculated modes of axle subframe for V1-steel variant are shown in Fig. 6.
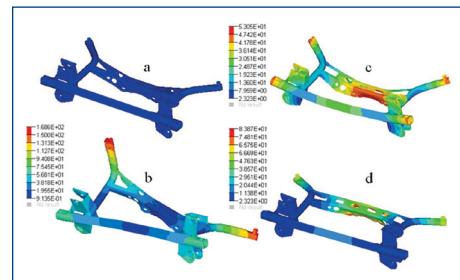
Figure 6. First three natural modes V1-steel, a – undeformed state, b – first natural mode (torque), c -second natural mode (bend), d – third self mode (bend)
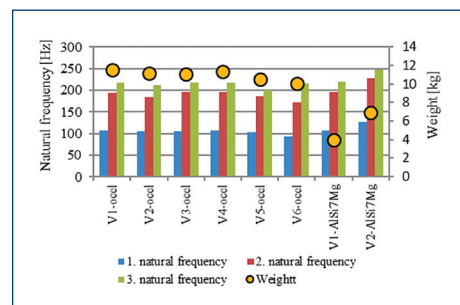
Figure 7. Comparison of first three natural-frequencies and weight for analyzed variants

Each mode corresponds to the frequency. The first natural frequency value was calculated 106 Hz (torsion), the second frequency of 193 Hz (bending) and the third frequency 218 Hz (bending). The natural frequencies of the other variations of the axle subframe are compared in Fig. 7.

3.2 MBS model with implemented flexible models
The subframe flexible model is linked to MBS model through RBE2 spiders, which represent the interface between kinematic points of MBS model and corresponding nodes of subframe flexible model (Fig. 8).
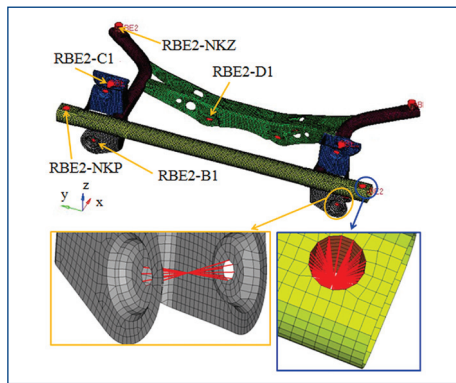
Figure 8. RBE2 points of subframe flexible model with details on RBE2

Point RBE2-B1 linking kinematic point B1 (node number 24496) with 16 nodes of holes for connecting the arm 3. RBE2-C1 connects the point C1 (24498) with 24 nodes of holes for arm 4. RBE2-D1 links point D1 (24500) with 20 nodes of hole for arm 5. RBE2-NKP point links point NKP (24490) with 154 nodes of frontal subframe bush and RBE2-NKZ connecting the point NKZ (24492) with 152 nodes of rear subframe bush. Similarly spiders RBE2-A1, RBE2-A2b and RBE2-A2t were created for longitudinal arms.

4. PROCESSING OF SIMULATION ANALYSES
The MotionSolve module was used for calculations of elasto-kinematic properties of assembled MBS model. Three loading modes were defined. The first mode loads the absolutely rigid wheel support with vertical force that causes vertical movement of the wheel Wz (wheels travel from the lower to the upper stop). The interval for wheel movement was set $W_Z = (-105; 105)$ mm. The second and third mode load the wheel support with lateral and longitudinal force, generated during vehicle braking and turning. Lateral force was in the interval FL = (−10 000; 10 000) N, and longitudinal braking force in the interval FB = (0; 10 000) N. Furthermore, the tyre properties wheelbase and center of gravity of the vehicle were defined in MotionSolve module. Calculations were carried out with the time step of 0.05 s in the interval from 0 s to 80 s.

5. VALIDATION OF MBS COMPUTATIONAL MODEL
The resulting values of the MBS simulation model were validated by experimental measurements. Testing machine Beissbarth VAG 1995 (Fig. 9) was used for this purpose.
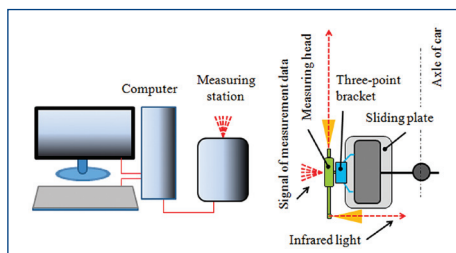
Figure 9. Principle of measuring device Beissbarth VAG 1995

The waveforms of toe angle α and camber angle β in the dependence on the wheel travel Wz were measured. Testing machine was equipped with measuring head containing two CDD cameras that detect the geometric position of the wheel using infrared radiation. Measured vehicle was fixed to measuring devices and measuring heads were set in horizontal position. After calibration of the testing device the vehicle loading and unloading was measured so that the center of the rear wheel W is in the range $W_Z = (-100; 100)$ mm. Measuring step has been chosen 10 mm.

The output of measurements is the waveform of toe angle $\alpha = f (W_Z)$ and camber angle $\beta = f (W_Z)$ for each measured position of the wheel. This procedure was applied for the verification of results of the V1-steel design variant of flexible subframe.

6. SIMULATION RESULTS AND DISCUSSION
Output data from the simulation calculations in MotionSolve were further analyzed and processed in the postprocessors HyperGraph and HyperView.

6.1 Effect of subframe flexibility during wheel vertical movement
The dependencies of toe angle α and camber angle β on the wheel center vertical movement Wz belong to the basic indicators in the analysis of elasto-kinematic properties of single-axle suspension. Calculated dependencies of $\alpha = f (W_Z)$ in Fig. 10 and $\beta = f (W_Z)$ in Fig. 11 show that the effect of subframe flexibility in the MBS model affects especially the toe angle values. The camber course differs only minimally. Negative values indicate negative camber. The investigated design variants of flexible axle also affect only the toe angle. Dependencies of toe angle $\alpha = f (W_Z)$ have the shape of an inverted S, with approximately linear portion interval $W_Z = (-30, 30)$ mm. Toe angle of basic variant of flexible subframe V1-steel differs from the rigid model for different wheel positions. The difference for the wheel position Wz = −30 mm and Wz = 30 mm is 15.6 % and 5.9 % for the position Wz = −72 mm and Wz = 72 mm it is 33 % and 22%.
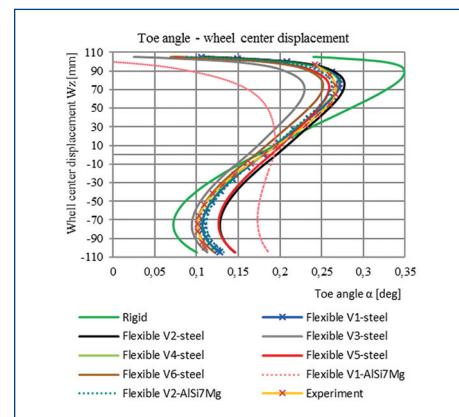
Figure 10. α = f (WZ) for rigid and flexible model of subframe
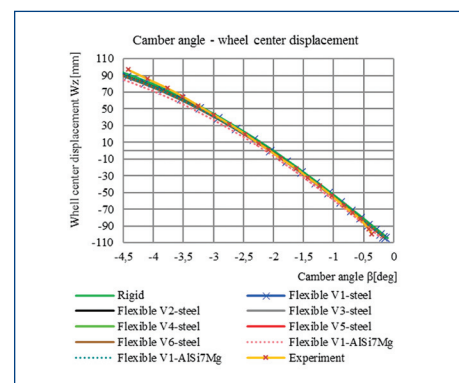
Figure 11. β = f (WZ) for rigid and flexible model of subframe

It was investigated that analyzed subframe variants influence the slope of the linear part of wheel toe characteristics. The tangent slope for rigid subframe is 0.48 in variant V1-steel and 0.71 in variant V2-AlSi7Mg. Variant V2-AlSi7Mg has similar toe characteristics as the default variant V1-steel but enables interesting weight saving of 4.7 kg. Calculated waveforms for the suspension with steel subframe V1-steel conform very well to the experimental measurement.

6.2 Effect of subframe flexibility during lateral and longitudinal loading

The effect of subframe flexibility on geometrical parameters of wheel suspension during loading by lateral force is shown in Figs. 12 and 13. The individual variants of subframe flexible model and the rigid model are there graphically compared.
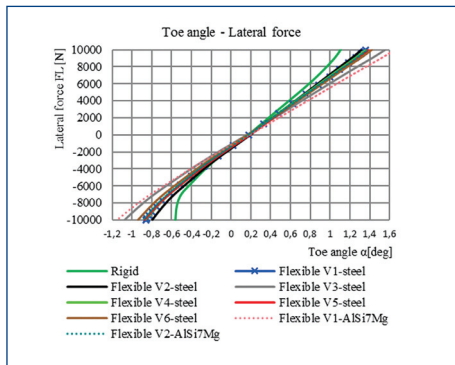
Figure 12. α = f (FL) for rigid and flexible model of subframe
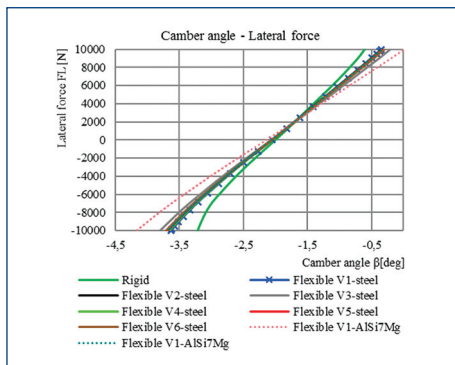
Figure 13. β = f (FL) for rigid and flexible model of subframe

Toe and camber angle are increasing linearly with the lateral force FL, which results in stable driving behavior in a curve. When the force of suspension load reaches FL = 4 800 N the toe angle for rigid model changing the value of α = 0.67 deg. For the flexible model the toe value is higher by 9.12 %. The camber angle changes during this type of loading to the value β = −1.29 deg for the rigid model, and β = −1.21 deg for the flexible model.

Elasto-kinematic behavior of suspension under the action of the longitudinal braking force FB shows dependencies α = f (FB) in Fig. 14 and β = f (FB) in Fig. 15.

When increasing the load to FB = 1 250 N the wheel toe also increases and wheel camber decreases. After the break value the wheel toe linearly decreases and on the contrary the wheel camber increases. Toe and camber angle changing by longitudinal force FB = 4 800 N for the rigid model of subframe α = 0.12 deg and β = − 2.06 deg and for the flexible model of subframe to α = 0.02 deg and β = −2.13 deg. The differences in results between rigid and flexible model of subframe increasing linearly with the loading value.

Changes in geometrical parameters of the linear section of the dependency related to 1 kN of lateral force FL and longitudinal force
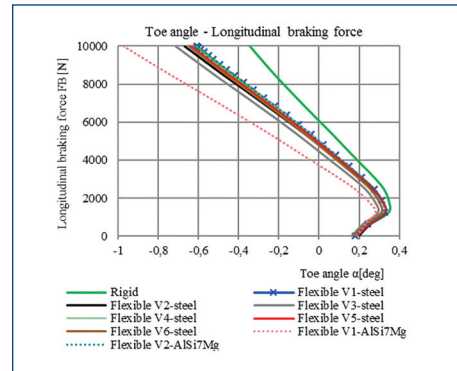
Figure 14. α = f (FB)for rigid and flexible model of subframe
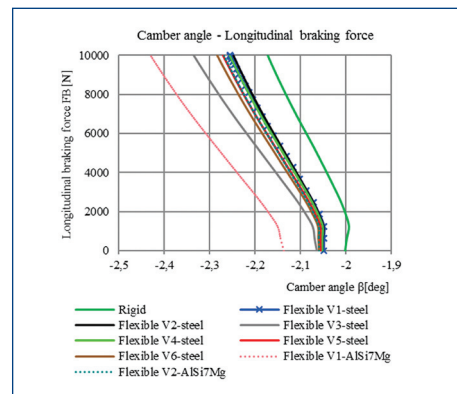
Figure 15. β = f (FB) for rigid and flexible model of subframe
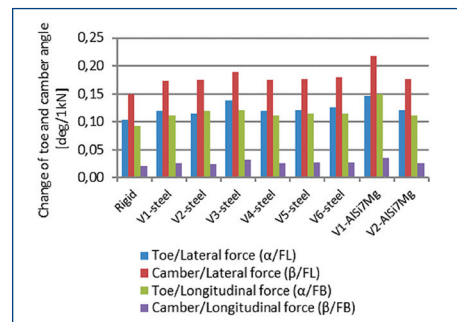
Figure 16. Changes of geometrical parameters during force loading

FB are summarized in Fig. 16. In general it was investigated that for this type of suspension the force load mostly changes the camber angle, especially during action of lateral forces.

For the rigid model of subframe there are always the lowest changes in the toe and camber angle compared to the variants with flexible model. The highest change can be observed in variant V1-AlSi7Mg which is material alternative to model V1-steel. High effect can also be found in modification of plate thickness (3) for joining the arm 3 in variant V3-steel then in thickness of the transverse tube (2), variant V6-steel. On the contrary, the minimal influence was calculated in variant V2-steel with modified thickness of the rear crossbar (5). Variant V2-AlSi7Mg gives similar results as basic variant V1-steel and enables weight saving. Different values of geometric parameters primarily wheel camber values of individual variants under force load FB = 0 N are caused by the vertical load of the suspension caused by vehicle mass.

7. CONCLUSION

This paper deals with the effect of subframe flexibility on elasto-kinematic properties of single-axle suspension. For this purpose the MBS model of suspension was prepared in MotionView module of HyperWorks.

This model includes not only non-linear deformation characteristics of rubber-metal bushings of individual suspension arms but also the power elements like springs, shock absorbers and transverse stabilizer. These elements ensure the proper setup of simulation model and make calculations more accurately. Furthermore, the FEM model of subframe consisting of 24238 elements in eight construction variants with AlSi7Mg and steel was created in Hypermesh module. Individual models were enhanced by the RBE2 elements using modal synthesis of natural modes Craig-Bampton. Flexible models were then linked to the MBS model. Elasto-kinematic analyses showed that the flexible model of subframe in comparison to rigid model primarily influences the course of wheel toe in the vertical movement of the wheel center and toe and camber angle under the effect of longitudinal and lateral forces. The basic variant of the model shows results validated by experimental measurements. Compared to the basic variant V1-steel, the highest influence on the elasto-kinematic characteristics during loading was found in variant V3-steel with modified thickness of the bracket (3). The results show that the use of the calculation model includes the flexibility of the suspension subframe improves elasto-kinematic analysis. Therefore, we should include the flexibility of other supporting elements such as knuckle or transverse arms.

REFERENCES

[Altair 2015] Altair, Practical Aspect of Multi-Body Simulation with Hyperworks [online], Michigan, January 2015 [cit 10/09/2015]. Available on: http://cdn2.hubspot.net/hub/47251/file-2400445158-pdf/docs/MBD_StudyGuide_Book_Januar2015.pdf?t=1423864156167&utm_source=hs_automation&utm_medium=email&utm_content=15646418&_hsenc=p2ANqtz-8ikosxeHUQ3ikxJb4GjEiCvCZPf9nqp-oK0m0o5j9iAKyF51wpavH4_sRIu9QxVmOiJvt2NblipauTqaRKPnpVsV_z9w&_hsmi=15646460

[Brat 1981] Brat, V. Matrix methods in analysis and synthesis of shape mechanical systems, Prague: Academia, 1981. (in Czech)

[Heissing 2008] Heissing, B., Ersoy, M. Fahrwerkhandbuch, Wiesbaden: Vieweg+Teubner Verlag, 2008. ISBN 978-3-8348-0444-0

[Hiller 1985] Hiller, M., Woernle, C. Elastokinematicsal analysis of a five-point wheel suspension. Revue de la SIA Ingenieurs de l'Automobile, 1985; pp 77-80.

[Knapczyk 1995] Knapczyk, J., Dzierzek, S. Displacement and force analysis of five-rod suspension with flexible joints. Trans. ASME, Journal of Mechanical Design, 1995, No.117, pp 532-538. ISSN 1528-9001

[Knapczyk 2006a] Knapczyk, J., Maniowski, M. Elastokinematics modeling and study of five-rod suspension with Subframe, Mechanism and Machine Theory, 2006, Vol.41, pp 1031–1047. ISSN 0094-114X

[Knapczyk 2006b] Knapczyk, J., Maniowski, M. Stiffness synthesis of a five-rod suspension for given load displacement characteristics. Proceedings of the Institution of Mechanical Engineers, 2006, Vol. 220, pp 879-889. ISSN 09544062.

[Michalec 1995] Michalec, J., et al. Flexibility and strength I, Prague: CTU in Prague, 1995. ISBN 8001013332 (in Czech)

[Moon 2012] Moon, I. D., Oh, C. Y. Computational model for analyzing the kinematics and flexibility characteristics of a commercial vehicle's front suspension system. International Journal of Automotive Technology, 2012, Vol. 13, No. 2., pp 279-284. ISSN 1229-9138. DOI 10.1007/s12239-012-0025-4

[Popp 2010] Popp, K., Schiehlen, W. Ground Vehicle Dynamics. Berlin Heidelberg: Springer – Verlag, 2010, ISBN 978-3-540-24038-9, DOI 10.1007/978-3-540-68553-1

[Shim 2010] Shim, T., Velusany, P.C. Improvement of vehicle roll stability by varing suspension properties. International Journal of Vehicle System Dynamics, 2010, Vol. 49, No. 1–2., pp 129–152. ISSN 0042-3114 (Print). ISSN 1744-5159 (Online). DOI 10.1080/00423111003615196

[Simionescu 2002] Simionescu, P. A., Beale, D. Synthesis and analysis of the five-link rear suspension system used in automobiles. Mechanism and Machine Theory, 2002, Vol. 37, pp 815–832. ISSN 0094–114X

[Stejskal 2001] Stejskal, V., et al. Mechanics III, Prague: CTU in Prague, 2001. ISBN 80-01-00918-1 (in Czech)

CONTACTS

Ing. Tomas Vrana
CULS Prague, Faculty of Engineering
Department of Vehicles and Ground Transport
Kamycka 129, 165 21 Prague 6 – Suchdol, Czech Republic
e-mail: vrana.ds@seznam.cz
www.tf.czu.cz

prof. Ing. Jan Kovanda, CSc.
CTU in Prague, Faculty of Transportation Sciences
Department of Security Technologies and Engineering
Konviktska 20, 110 00 Prague 1, Czech Republic
tel.:+420 224 359 613, e-mail: kovanda@fd.cvut.cz,
www.fd.cvut.cz

Ing. Josef Bradac, PhD.
Skoda Auto University, Department of Automotive Technology
Na Karmeli 1457, 293 60 Mlada Boleslav, Czech Republic
tel.:+420 326 823 038, e-mail: Josef.Bradac@savs.cz,
www.savs.cz